

PHYSICAL REVIEW C

NUCLEAR PHYSICS

THIRD SERIES, VOLUME 50, NUMBER 4

OCTOBER 1994

RAPID COMMUNICATIONS

The Rapid Communications section is intended for the accelerated publication of important new results. Manuscripts submitted to this section are given priority in handling in the editorial office and in production. A Rapid Communication in *Physical Review C* may be no longer than five printed pages and must be accompanied by an abstract. Page proofs are sent to authors.

Electric form factor of the neutron from the ${}^2\text{H}(\vec{e}, e' \vec{n}){}^1\text{H}$ reaction at $Q^2 = 0.255 \text{ (GeV}/c)^2$

T. Eden,^{1,*} R. Madey,^{1,2} W.-M. Zhang,¹ B. D. Anderson,¹ H. Arenhövel,³ A. R. Baldwin,¹ D. Barkhuff,⁴ K. B. Beard,^{5,2} W. Bertozzi,⁶ J. M. Cameron,⁷ C. C. Chang,⁸ G. W. Dodson,⁶ K. Dow,⁶ M. Farkhondeh,⁶ J. M. Finn,⁵ B. S. Flanders,⁹ C. Hyde-Wright,^{11,†} W.-D. Jiang,¹¹ D. Keane,¹ J. J. Kelly,⁸ W. Korsch,^{6,‡} S. Kowalski,⁶ R. Lourie,⁴ D. M. Manley,¹ P. Markowitz,^{5,§} J. Mougey,^{10,||} B. Ni,^{7,¶} T. Payerle,⁸ P. J. Pella,¹² T. Reichelt,¹³ P. M. Rutt,^{5,**} M. Spraker,⁷ D. Tieger,⁶ W. Turchinets,⁶ P. E. Ulmer,^{10,†} S. Van Verst,⁴ J. W. Watson,¹ L. B. Weinstein,^{6,†} and R. R. Whitney¹⁰

¹Kent State University, Kent, Ohio 44242

²Hampton University, Hampton, Virginia 23668

³Johannes Gutenberg-Universität, D-55099 Mainz, Germany

⁴University of Virginia, Charlottesville, Virginia 22904

⁵College of William and Mary, Williamsburg, Virginia 23185

⁶Massachusetts Institute of Technology and Bates Linear Accelerator Center, Cambridge, Massachusetts 02139

⁷Indiana University Cyclotron Facility, Bloomington, Indiana 47405

⁸University of Maryland, College Park, Maryland 20742

⁹The American University, Washington, D.C. 20016

¹⁰Continuous Electron Beam Accelerator Facility, Newport News, Virginia 23606

¹¹University of Washington, Seattle, Washington 98195

¹²Gettysburg College, Gettysburg, Pennsylvania 17325

¹³Physikalisches Institut Universität Bonn, D-53115 Bonn, Germany

(Received 16 May 1994)

We determined the electric form factor G_E^n of the neutron from the quasielastic ${}^2\text{H}(\vec{e}, e' \vec{n}){}^1\text{H}$ reaction at a central squared four-momentum transfer $Q^2 = 0.255 \text{ (GeV}/c)^2$ with a longitudinally polarized electron beam of 868 MeV and a low ($\sim 0.8\%$) duty factor. A neutron polarimeter designed and constructed specifically for this experiment was used to measure the sideways polarization of the recoil neutron, which was detected in coincidence with the scattered electron. Theoretical calculations have established that this polarization-transfer technique for quasielastic scattering produces a value of G_E^n that shows little sensitivity to the influence of final-state interactions, meson-exchange currents, isobar configurations, and deuteron structure. The value for G_E^n from this measurement is $0.066 \pm 0.036 \pm 0.009$.

PACS number(s): 25.30.Fj, 13.40.Gp, 14.20.Dh, 25.10.+s

* Present address: Hampton University, Hampton, VA 23668.

† Present address: Old Dominion University, Norfolk, VA 23529.

‡ Present address: California Institute of Technology, Pasadena, CA 91125.

§ Present address: University of Maryland, College Park, MD 20742.

|| Present address: Centre d'Etudes Nucléaires, Saclay, Gif-sur-Yvette, France.

¶ Present address: Rush University, Chicago, IL 60612.

** Present address: Rutgers University, Piscataway, NJ 08855.

The electric form factor G_E^n of the neutron is a fundamental quantity for the understanding of both nucleon and nuclear structure. The dependence of G_E^n on Q^2 , the squared four-momentum transfer, is determined by the charge distribution within the neutron. The value for G_E^n is small and poorly known for all Q^2 except for the slope at $Q^2=0$, which was obtained to $\sim 2\%$ statistical accuracy by scattering neutrons from atomic electrons [1]; however, the relationship between the neutron-electron scattering length and the slope of G_E^n suffers from a 20% model dependence that occurs when resonance corrections are applied [2]. Away from $Q^2=0$, information on G_E^n has been obtained from elastic and quasielastic electron-deuteron scattering. Results from elastic electron-deuteron scattering, where G_E^n is extracted indirectly from the charge structure function $A(Q^2)$ of the deuteron for $Q^2 < 0.75$ (GeV/c)², depend on the choice of deuteron wave functions [3,4]. Recent results from a Rosenbluth separation of quasielastic electron-deuteron scattering cross sections at $Q^2 \geq 1.75$ (GeV/c)² yielded values of $(G_E^n)^2$ consistent with zero where the effects of final-state interactions (FSI) and meson-exchange currents (MEC) may be important and remain to be investigated [5]. With the recent advent of polarized electron beams and polarized nuclear targets, a new realm for obtaining information about the charge structure of the neutron commenced. Initial measurements [6,7] of asymmetries in inclusive quasielastic scattering of polarized electrons from polarized ³He have large uncertainties; extraction of G_E^n from the polarized neutron requires knowledge of the nuclear structure of the polarized ³He [8]. Recently, the Mainz A3 Collaboration reported two asymmetry measurements [9,10] obtained separately from the quasielastic ²H($\vec{e}, e'\vec{n}$)¹H and ³He($\vec{e}, e'\vec{n}$) reactions. A positive value for G_E^n was extracted by measuring the asymmetry ratio A_{\perp}/A_{\parallel} at $Q^2=0.31$ (GeV/c)² from the exclusive ³He($\vec{e}, e'\vec{n}$) reaction [10]. The analyzing power of the neutron polarimeter used by the A3 Collaboration in the ²H($\vec{e}, e'\vec{n}$)¹H reaction remains to be measured before a reliable value of G_E^n can be extracted.

This Rapid Communication reports an initial experimental determination of G_E^n from the exclusive quasielastic ²H($\vec{e}, e'\vec{n}$)¹H reaction. The special advantage of this polarization-transfer measurement on the deuteron is that theoretical calculations predict the result to be insensitive to FSI, MEC, isobar configurations, and the choice of deuteron wave functions [11–14]. To determine G_E^n , we employ the technique suggested by Arnold, Carlson, and Gross [15] whereby G_E^n is extracted by measuring the polarization of the recoil neutron after quasielastic scattering of a longitudinally polarized electron from an unpolarized neutron. For a polarized electron beam with measured longitudinal polarization P_L , the sideways component $P_{S'}$ of the neutron polarization normal to the three-momentum transfer \vec{q} is given by $P_{S'} = P_L D_{LS'}$ [16], where the polarization-transfer coefficient $D_{LS'}$ is related to G_E^n . For a free neutron [15], we have

$$\begin{aligned} I_0 D_{LS'} &= -2(G_M^n G_E^n) [\tau(1+\tau)]^{1/2} \tan(\theta_e/2) \\ &\equiv -(G_M^n G_E^n) K_1(\theta_e, Q^2), \end{aligned} \quad (1)$$

with

$$\begin{aligned} I_0 &= (G_E^n)^2 + (G_M^n)^2 \tau [1 + 2(1+\tau) \tan^2(\theta_e/2)] \\ &\equiv (G_E^n)^2 + K_2(\theta_e, Q^2) (G_M^n)^2, \end{aligned} \quad (2)$$

where G_M^n is the magnetic form factor of the neutron, $\tau = Q^2/4M^2$ with M the nucleon mass, and θ_e is the electron scattering angle. From Eqs. (1) and (2), we find

$$D_{LS'} = \frac{-(G_E^n/G_M^n) K_1(\theta_e, Q^2)}{K_2(\theta_e, Q^2) + (G_E^n/G_M^n)^2}; \quad (3)$$

thus, a measurement of $D_{LS'}$ yields the ratio G_E^n/G_M^n .

The experiment was performed in the Spring of 1991 at the Bates Linear Accelerator Center. Longitudinally polarized electrons were used to disintegrate deuterons in an unpolarized liquid deuterium (LD₂) target with a diameter of 5 cm along the direction of the beam. From luminosity studies, the maximum variation of the target density was observed to be $\sim 1\%$. Longitudinally polarized electrons were produced by photoemission from a GaAs crystal excited by circularly polarized laser light from an electro-optically shuttered continuous-wave krypton-ion laser. The design of the polarized-electron gun is similar to one used at SLAC [17] and was modified to match the demands of the higher Bates injection energy. A beam energy of 868 MeV was achieved by recirculating the beam. This energy was chosen so that the electron polarization, after passing through the recirculator and the transport system, was parallel (or antiparallel) to the final electron momentum. We detected the quasielastically scattered electrons (centered at a momentum of 730 MeV/c) with the One-Hundred-Inch Proton Spectrometer (OHIPS) [18], which is a 90° vertical-bend quadrupole-quadrupole-dipole spectrometer, positioned at 37.0° to the right of the incident beam. The solid angle acceptance for the spectrometer was 5.6 msr and the momentum acceptance was ± 32 MeV/c. Recoil neutrons were detected in coincidence with the scattered electrons. A neutron polarimeter constructed specifically for this experiment [19] was used to perform the polarization analysis of the recoil neutrons. The neutron polarimeter was positioned at the angle of \vec{q} (viz., 57.0° to the left of the incident beam) and was housed in a large shielding enclosure composed of a 1-m-thick front steel wall with a 26.7-cm-high \times 65.8-cm-wide collimated opening with a lead-steel wall situated behind the collimated opening (ahead of the polarimeter) comprised of 10.16-cm lead bricks sandwiched between two 3.125-cm steel plates; the rest of the shielding enclosure consisted of 122-cm-thick walls and a 61-cm-thick roof of reinforced high-density ($\rho = 3.9$ g/cm³) concrete. The polarimeter consisted of 12 scintillation counters—four mineral oil (BC-517L) primary scatterers (0.254 m high \times 0.508 m long \times 0.102 m thick) and two sets of four rear plastic (NE-102) analyzer detectors (0.508 m high \times 1.016 m long \times 0.102 m thick). The rear detectors, positioned above and below the nominal scattering plane, were located at a polar angle $\theta = 21^\circ$ with respect to the direction of \vec{q} . The mean flight path between the midpoint of the front detector array and the midpoint of each rear detector array was 2 m. The solid angle acceptance for the neutron polarimeter was 9.68 msr. The neutron polarimeter was calibrated at the Indiana University Cyclotron Facility by measuring the average analyzing power $\langle A_y \rangle$ for the $0^+ \rightarrow 0^+$ isobaric

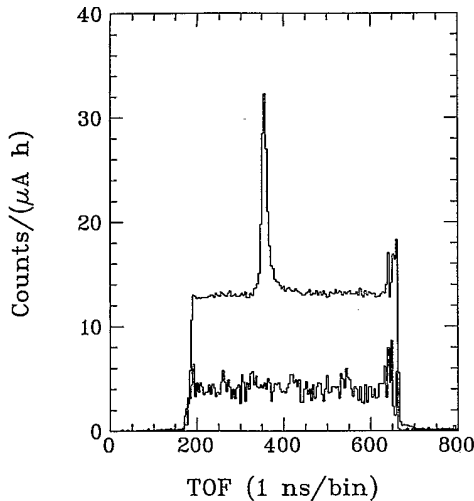


FIG. 1. Summed triple-coincidence TOF spectra after all software cuts for the ${}^2\text{H}(\vec{e}, e'\vec{n}){}^1\text{H}$ reaction with a background level at 12 counts/($\mu\text{A h}$) and for the ${}^1\text{H}(\vec{e}, e'X)$ reaction (normalized to LD_2) with a background level at ~ 4 counts/($\mu\text{A h}$).

analog state in the ${}^{14}\text{C}(\vec{p}, \vec{n}){}^{14}\text{N}$ reaction at 0° ; the result for $\langle A_y \rangle$ is $(38.2 \pm 4.3)\%$ [20]. The polarization P_L of the incident electron beam was measured with a Møller polarimeter in the coincidence mode; the result for P_L is $(42.4 \pm 1.8)\%$. This result does not include a correction, discussed by Levchuk [21], for the loss of events that results from the Fermi momentum of electrons in the polarized target. The configuration of the Møller polarimeter was described by Arrington *et al.* [22].

Usable data were obtained from 544 $\mu\text{A h}$ of an integrated beam with a duty factor of 0.8% at an average beam current of approximately 1.8 μA , which corresponds to an average luminosity of $5.8 \times 10^{36} \text{ cm}^{-2} \text{ s}^{-1}$. Shown in Fig. 1 are two time-of-flight (TOF) spectra [normalized to counts/($\mu\text{A h}$)] for coincidence events between the neutron polarimeter and the electron spectrometer after imposing final software cuts. The coincidences were generated by detecting an electron in OHIPS in coincidence with a neutron in a front detector of the polarimeter, gated by an event in one of the rear detectors of the polarimeter. Charged-particle events were vetoed in hardware by thin paddle scintillators positioned immediately ahead of each neutron detector array. The spectrum with a coincidence peak sitting on a background level at 12 counts/($\mu\text{A h bin}$) comes from the entire LD_2 data set. A shadow-shield run with the LD_2 target revealed that the background level was reduced to ~ 1 count/($\mu\text{A h bin}$). The relatively flat spectrum at a background level of ~ 4 counts/($\mu\text{A h bin}$) from LH_2 (normalized to LD_2) reveals a contribution of about 30% to the background from neutrons produced by (p, n) reactions in the lead-steel wall between the target and the polarimeter. Contamination under the $(e, e'n)$ coincidence peak from the two-step process ${}^2\text{H}(e, e'p) + (p, n)$ in the lead-steel wall was found to be less than 1% from a fit to the LH_2 spectrum with parameters obtained from a fit to the LD_2 spectrum in Fig. 1. Contamination from the two-step process $(e, e'p) + {}^2\text{H}(p, n)$ within the LD_2 target cell was calculated to be negligible

($< 0.03\%$) based on known $(e, e'p)$ cross sections and the measured (p, n) cross sections of Langsford *et al.* [23].

Threefold coincidence spectra were summed over both helicity states and over neutrons scattered either up or down. To measure the scattering asymmetry ξ , the LD_2 spectrum must be decomposed into four TOF spectra—an up and a down spectrum for each helicity state; then $D_{LS'}$ was determined from

$$D_{LS'} = \frac{P_{S'}}{P_L} = \frac{\xi}{\langle A_y \rangle P_L} = \frac{1}{\langle A_y \rangle P_L} \left(\frac{r-1}{r+1} \right), \quad (4)$$

where $\langle A_y \rangle$ is the analyzing power of the polarimeter and the cross ratio r is

$$r \equiv \left[\frac{N_T^+ N_B^-}{N_B^+ N_T^-} \right]^{1/2}. \quad (5)$$

Here N_B^+ (N_T^+) and N_B^- (N_T^-) denote the number of events scattered to the bottom (top) detectors of the polarimeter with longitudinal polarization of the incident electrons parallel (+) and antiparallel (−), respectively, to the electron momentum. In this cross-ratio method of analysis, false asymmetries from helicity-dependent errors in charge integration or system deadtimes or from errors in detection efficiency and acceptances cancel to all orders, whereas false asymmetries from misalignments with respect to \vec{q} or to differences in the beam polarization for the two helicity states cancel to first order [24].

Events that could contaminate the coincidence peak in Fig. 1 were of special interest. Correlated electron-front detector coincidences with associated uncorrelated rear detector events (event “U”) could dilute the correlated electron-front-rear detector real event signal (event “C”). The scattering asymmetry ξ is diluted by a factor R_d given by

$$R_d = \left(1 + \frac{N_U}{N_C} \right)^{-1}, \quad (6)$$

where N_U , the number of uncorrelated events, was extracted from the secondary-scattering time-of-flight (ΔTOF) spectra in the neutron polarimeter. The ΔTOF spectra were generated by a coincidence between the front and rear detectors in the polarimeter, where the time difference between the front and rear interactions is the recorded flight time of the scattered neutron. The final event selection yielded a true scattering asymmetry $\xi_t = \xi/R_d = (2.0 \pm 1.0)\%$ with $R_d = (77.3 \pm 1.3)\%$ and $D_{LS'} = (12.3 \pm 6.2)\%$. Using Eq. (3) with $G_M^n = 1.060 \pm 0.039$ [25], we obtained $G_E^n = 0.066 \pm 0.036 \pm 0.009$. The scale uncertainty (± 0.009) includes systematic and statistical contributions from our independent measurements of $\langle A_y \rangle$, P_L , and G_M^n and a theoretical uncertainty (based on Arenhövel’s model) of $\pm 2.9\%$ averaged (with the code MCEEP [26]) over the experimental acceptances. This theoretical uncertainty decreases with increasing Q^2 .

Shown in Fig. 2 is the value of G_E^n extracted from this measurement (Bates E85-05) compared with the data and parametrization of Platchkov *et al.* [4], which depend on the choice of the N - N potential used in extracting G_E^n from $A(Q^2)$. Extraction of G_E^n from elastic electron-deuteron scat-

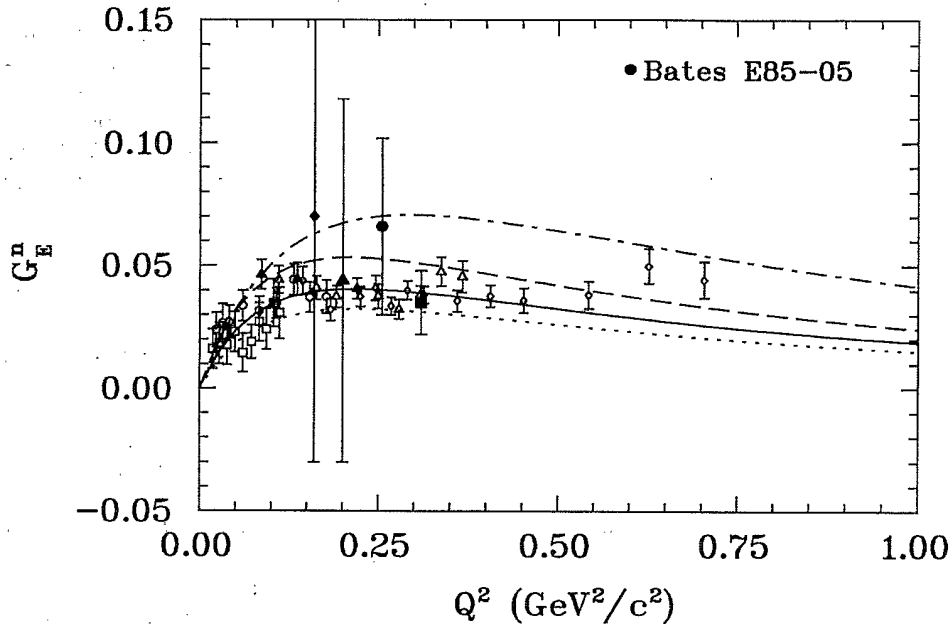


FIG. 2. The value of G_E^n (shaded circle) extracted from the quasielastic ${}^2\text{H}(\vec{e}, e'n){}^1\text{H}$ reaction is compared to the parametrization [4] $G_E^n(Q^2) = -a\mu_n\tau G_D(1+b\tau)^{-1}$, where $G_D = [1+Q^2/0.71(\text{GeV}/c)^2]^{-2}$ and a and b depend on the choice of N - N potential: Nijmegen (dash-dotted), Argonne V14 (dashed), Paris (solid), and Reid soft core (dotted). The open squares, circles, triangles, and diamonds represent the data from Platchkov *et al.* [4] extracted with the Paris potential. The other three points are results for G_E^n extracted from the inclusive ${}^3\text{He}(e, e')$ reaction by Woodward *et al.* [6] (shaded diamond) and Thompson *et al.* [7] (shaded triangle) and from the exclusive ${}^3\text{He}(e, e'n)$ reaction by Meyerhoff *et al.* [10] (shaded square).

tering, which was used by Platchkov *et al.*, is limited to $Q^2 < 1.0$ $(\text{GeV}/c)^2$. Figure 3 compares some recent G_E^n data (omitting the Platchkov data for clarity) with various parametrizations of G_E^n . An early version of the Gari-

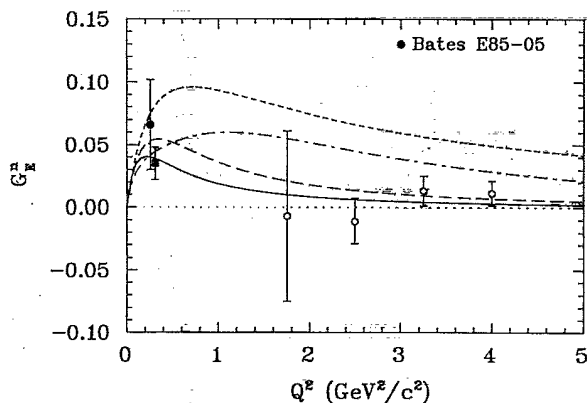


FIG. 3. Recently reported values of G_E^n are compared to various parametrizations of G_E^n . The data points are from the quasielastic ${}^2\text{H}(\vec{e}, e'n){}^1\text{H}$ reaction (shaded circle), the exclusive ${}^3\text{He}(\vec{e}, e'n)$ reaction by Meyerhoff *et al.* [10] (shaded square), and the inclusive quasielastic ${}^2\text{H}(e, e')$ results of Lung *et al.* [5] (open circles) [Note that we preserve the sign of $(G_E^n)^2$ when converting to G_E^n for the Lung data points.] The parametrizations are from the work of Galster *et al.* [3] $G_E^n = -\tau\mu_n G_D(1+5.6\tau)^{-1}$ (long dashes); Platchkov *et al.* [4], where the Paris potential fit is shown (solid); the Gari-Krumpelmann [28] vector meson dominance-perturbative QCD model 3 (dash-dotted); and the parametrization $G_E^n = -\tau G_M^n$ (short dashes), where $F_{1n} = 0$.

Krumpelmann model [27], which is based on a synthesis of vector-meson dynamics at low Q^2 and the asymptotic predictions of perturbative QCD at high Q^2 , suggested that the neutron Dirac form factor $F_{1n} \sim 0$, implying that $G_E^n \sim -\tau G_M^n$. More recently [28], Gari and Krumpelmann included ϕ -meson couplings to the nucleon and reconsidered the scale parameter that governs suppression of the Pauli form factor (F_{2n}) from quark helicity flip. Their revised model predicts that G_E^n near $Q^2 \sim 1$ $(\text{GeV}/c)^2$ is sensitive to the strange-quark content of the neutron; more precise measurements are necessary to test this prediction. Gari and Krumpelmann's revised prediction for G_E^n is shown as the dash-dotted curve in Fig. 3.

Although the measurement reported here was limited by the statistical uncertainty and the signal-to-background ratio, this measurement demonstrates the feasibility of the technique for extracting G_E^n from the quasielastic ${}^2\text{H}(\vec{e}, e'n){}^1\text{H}$ reaction. These limitations will be removed in future experiments [29] with high duty-factor accelerators. The scale uncertainty from the uncertainties in $\langle A_y \rangle$ and P_L can be reduced by measuring the ratio of the scattering asymmetries for the longitudinal and sideways components of the neutron polarization [30]. Measurements at CEBAF with a luminosity of $3.2 \times 10^{38} \text{ cm}^{-2} \text{ s}^{-1}$ and a duty factor of 100% promise high-precision ($\Delta G_E^n < 0.01$) determinations of G_E^n that will distinguish between various models of G_E^n and reduce theoretical uncertainties in calculations that depend on G_E^n .

We thank the Bates staff for their generous work during all phases of this experiment, Professor B. Mosconi for providing his results, and Dr. S. K. Platchkov for providing his G_E^n results extracted with the Paris potential. This work was

supported in part by the National Science Foundation under Grant Nos. PHY-91-07064, HRD-91-54090, PHY-91-12816, PHY-89-02479, PHY-88-02392, PHY-86-58127, PHY-86-15512, PHY-85-01054, the Department of Energy under

Grant Nos. DE-FG05-90ER40570, DE-FG06-90ER40537, DE-FG02-89ER40531, DE-AC02-76ER03069, and by grants from the Deutsche Forschungsgemeinschaft (SFB 201 and RE 791/1-1).

- [1] V. E. Krohn and G. R. Ringo, *Phys. Rev.* **148**, 1303 (1966); L. Koester, W. Nistler, and W. Waschowski, *Phys. Rev. Lett.* **36**, 1021 (1976).
- [2] H. Leeb and C. Teichtmeister, *Phys. Rev. C* **48**, 1719 (1993).
- [3] S. Galster *et al.*, *Nucl. Phys.* **B32**, 221 (1971)
- [4] S. Platchkov *et al.*, *Nucl. Phys.* **A508**, 343c (1990); **A510**, 740 (1990).
- [5] A. Lung *et al.*, *Phys. Rev. Lett.* **70**, 718 (1993).
- [6] C. E. Woodward *et al.*, *Phys. Rev. C* **44**, R571 (1991).
- [7] A. K. Thompson *et al.*, *Phys. Rev. Lett.* **68**, 2901 (1992).
- [8] R.-W. Schulze and P. U. Sauer, *Phys. Rev. C* **48**, 38 (1993).
- [9] F. Klein *et al.*, in *The Workshop on Perspectives in Nuclear Physics at Intermediate Energies*, Trieste, 1993 (unpublished).
- [10] M. Meyerhoff *et al.*, *Phys. Lett. B* **327**, 201 (1994).
- [11] H. Arenhövel, *Phys. Lett. B* **199**, 13 (1987).
- [12] M. P. Rekaló, G. I. Gakh, and A. P. Rekaló, *J. Phys. G* **15**, 1223 (1989).
- [13] B. Mosconi, J. Pauschenwein, and P. Ricci, *Few-Body Systems*, Suppl. **6**, 223 (1992); private communication; T. Wilbois, G. Beck, and H. Arenhövel, *Few-Body Systems* **15**, 39 (1993).
- [14] J. M. Laget, *Phys. Lett. B* **273**, 367 (1991).
- [15] R. G. Arnold, C. E. Carlson, and F. Gross, *Phys. Rev. C* **23**, 363 (1981).
- [16] *Higher Energy Polarized Proton Beams*, Ann Arbor, Michigan, 1977, edited by A. D. Krisch and A. J. Salthouse, AIP Conf. Proc. No. 42 (AIP, New York, 1978), p. 142. (We change the notation from $K_{LS'}$ to $D_{LS'}$.)
- [17] C. Y. Prescott *et al.*, *Phys. Lett.* **77B**, 347 (1978).
- [18] R. S. Turley, Ph.D. Dissertation, MIT (1984).
- [19] R. Madey, A. R. Baldwin, P. J. Pella, J. Schambach, and R. M. Sellers, *IEEE Trans. Nucl. Sci.* **36**, 231 (1989).
- [20] T. Eden *et al.*, *Nucl. Instrum. Methods Phys. Res. Sect. A* **338**, 432 (1994).
- [21] L. G. Levchuk, *Nucl. Instrum. Methods Phys. Res. Sect. A* **345**, 496 (1994).
- [22] J. Arrington, E. J. Beise, B. W. Filippone, T. G. O'Neill, W. R. Dodge, G. W. Dodson, K. A. Dow, and J. D. Zumbro, *Nucl. Instrum. Methods Phys. Res. Sect. A* **311**, 39 (1992).
- [23] A. Langsford, P. H. Bowen, G. C. Cox, P. E. Dolley, R. A. J. Riddle, and M. J. M. Saltmarsh, *Nucl. Phys.* **A99**, 246 (1967).
- [24] G. G. Ohlsen and P. W. Keaton, Jr., *Nucl. Instrum. Methods* **109**, 41 (1973).
- [25] P. Markowitz *et al.*, *Phys. Rev. C* **48**, R5 (1993).
- [26] P. E. Ulmer, MCEP—Monte Carlo for Electro-Nuclear Coincidence Experiments, Report No. CEBAF-TN-91-101 (1991).
- [27] M. Gari and W. Krümpelmann, *Z. Phys. A* **322**, 689 (1985).
- [28] M. F. Gari and W. Krümpelmann, *Phys. Lett. B* **274**, 159 (1992); **282**, 483 (1992).
- [29] R. Madey *et al.*, Report No. CEBAF E93-038, 1993; Bates Report No. E89-04, 1989.
- [30] R. Madey *et al.*, Bates Proposal E89-04 update (1994).